Temperature effects in the vibrational spectra of self-assembled monolayers

Katrin Forster-Tonigold[a,b], Xia Stammer[c], Christof Wöll[c] and Axel Groß[a,b]
[a] *Helmholtz Institute Ulm (HIU) Electrochemical Energy Storage, D-89069 Ulm, Germany*
[b] *Institute of Theoretical Chemistry, Ulm University, D-89069 Ulm, Germany*
[c] *Institute of Functional Interfaces, Karlsruhe Institute of Technology, D-74800 Karlsruhe, Germany*

The vibrational spectrum of a thiolate-based self-assembled monolayer fabricated by adsorption of benzylmercaptan on an Au(111) substrate was studied using a combined experimental and theoretical approach employing infrared reflection absorption spectroscopy and density functional theory. The vibrational spectra were derived both using a finite diffences approach and from ab initio molecular dynamics simulations at various temperatures. In addition, the possibility of adsorbate-induced reconstructions of the Au(111) substrate has been taken into account. It turns out that the measured spectra can only be understood by taking finite temperatures into account.

PACS numbers: 68.43.Pq, 68.35.Ja, 68.43.Hn

In the past 30 years self-assembled monolayers (SAMs) have been established as model systems for various applications e.g. in the field of protective coatings, microanalysis or molecular electronics [1–4]. Insights into structures of SAMs and their formation have been obtained both by experiment and theory. Concerning theory, in particular density functional theory (DFT) calculations contributed to the understanding of SAMs [5–12]. Various structural sensitive experimental methods have been used for the characterization of thiolate-based SAMs on Au substrates, including scanning tunnelling microscopy (STM) and x-ray diffraction (XRD) [4]. In addition to microscopical and diffraction studies, vibrational spectroscopy, in particular based on infrared (IR) spectroscopy, has become an essential experimental tool which allows to infer information on the orientation and the structure of the thiolate molecules forming the SAM [4].

Although there are numerous experimental IR-studies, only few studies going beyond a comparison of experimental data with the vibrational spectrum of the isolated, single organothiol [13] have been reported. Since the strength of intermolecular interactions between the monomers forming a SAM can reach or even exceed that of the Au-S-bond anchoring the thiolate to the substrate, the embedding of the individual SAM-forming monomers in the surrounding 2D matrix of molecules has to be considered explicitly. Unfortunately, computational studies of the vibrational properties of a SAM in the context of slab-calculations represent a major effort because of the large size of the unit cell. Nevertheless, several papers have demonstrated that such studies are feasable [5–10]. However, to the best of our knowledge, computational studies have so far been restricted to 0 K, theoretical results for finite temperatures were not yet reported. Since experimental studies have revealed substantial changes in IR-data [14] when varying the temperature between 0 K and 300 K, the temperature where experimental SAM IR-spectra are typically recorded, theoretical studies at finite temperatures extending to room temperature are urgently required. In our combined theoretical and experimental study, we use SAMs formed by benzylmercaptan (BM) adsorbed on Au(111) as a model system. This system is well-characterized using scanning tunneling microscopy (STM) [15] as well as vibrational spectroscopy [13, 16, 17]. The results of our study clearly demonstrate that the measured spectra can only be understood if temperature effects are explicitly taken into account.

Periodic DFT calculations have been performed using the Vienna ab initio simulation package (VASP) [18]. Electron-electron exchange and correlation interactions have been described within the generalized gradient approximation (GGA) by employing the Perdew, Burke and Ernzerhof (PBE) functional [19]. In order to account for electron-ion interactions, the projector augmented wave (PAW) method [20, 21] has been used. The electronic one-particle wave functions were expanded in a plane wave basis set up to an energy cut-off of 400 eV. The metal surfaces were modeled by a slab consisting of five atomic layers that were separated by a vacuum region of 25 Å. The geometry of the adsorption complex was optimized by relaxing all atoms of the adsorbate and the metal atoms of the two uppermost layers of the surface.

The adsorption of BM radicals was modeled by a $(\sqrt{3}\times\sqrt{3})R30°$ overlayer structure as such a periodicity of the SAM has been found by STM experiments [15]. In addition, a larger $(3\times\sqrt{3})rect$ structure also corresponding to a $(2\sqrt{3}\times\sqrt{3})R30°$ overlayer containing two molecules per unit cell has been considered. $9\times9\times1$ and $4\times9\times1$ Monkhorst-Pack k point meshs with a Methfessel-Paxton smearing of 0.1 eV were used for the integration over the first Brillouin zone for the smaller and the larger overlayer structure, respectively.

In recent works it has been proposed that substrates supporting a thiolate-based SAM may not exhibit an ideal bulk-terminated Au(111) structure but in fact contain extra Au atoms [22, 23] or lack Au atoms in the uppermost surface layer [24]. In order to study the effect of adsorbate-induced reconstructions on the vibrational data, a set of calculations has also been carried out for

structures where the unit cell contains an extra Au atom or misses an Au atom. In the energy balance, the creation of such Au surface defects upon adsorption is accounted for by assuming that the Au atoms are in equilibrium with the bulk reservoir, resulting in the following expression for the adsorption energy:

$$E_{\mathrm{ad}}^{\mathrm{net}} = \frac{1}{n}(E_{\mathrm{tot}} - nE_{\mathrm{rad}} - E_{\mathrm{Au(111)}} - mE_{\mathrm{Au}}^{\mathrm{bulk}}), \qquad (1)$$

whereby n denotes the number of molecules and m the number of adatoms within the unit cell. For vacancy structures the number of missing Au atoms enters Eq. 1 as negative m. $\mathrm{E_{tot}}$, $\mathrm{E_{Au(111)}}$ and $\mathrm{E_{rad}}$ correspond to the total energy of the relaxed adsorption complex, the energy of the unreconstructed surface and the energy of the isolated radical, respectively. $E_{\mathrm{Au}}^{\mathrm{bulk}}$ denotes the cohesive energy of Au. Careful test studies that employ a dispersion correction scheme [25] showed that the relative stability order of the different structures does not change if van der Waals interactions are included. Therefore dispersion effects are not further discussed here.

Vibrational frequencies and normal modes were computed using two different methods. First, frequencies were derived from the Hessian matrix which was determined using the harmonic approximation within the finite difference approach. For each normal mode of vibration the IR intensity was calculated as the square of the derivative of the dipole moment. The dipole moment was calculated according to the correction scheme of Neugebauer *et al.* [26]. Only the dipole moment component along the surface normal was taken into account. In addition to the finite differences approach, infrared spectra were also determined directly from ab initio molecular dynamics (AIMD) simulations through Fourier Transform of the dipole autocorrelation function (FT-DACF) along trajectories of 10 ps run time with the first picosecond being regarded as thermalization period.

The SAMs were prepared by immersing clean Au(111) substrates in an ethanolic 1 mM BM (Fluka) ethanolic solution at room temperature (RT) for 20 h. After immersion the sample has been rinsed extensively with EtOH and dried under a nitrogen flow. The detailed pretreatment of the gold substrate as well as the commercial Vertex 80 FTIR spectrometer (Bruker Optics) were described elsewhere [9]. Spectra were recorded under ambient conditions (25°C) at a resolution of 2 $\mathrm{cm^{-1}}$.

According to the calculations, BM adsorbs preferably with the S-atoms positioned at a bridge position, slightly shifted towards the fcc hollow position with an Au-S distance of 2.03 Å and a S-C inclination angle of 56.6°. This adsorption configuration (see structure I of Fig. 1) has also been found in many other computational studies of thiolate adsorption on Au(111) [7, 8, 11, 27–30].

A comparison of the theoretical results obtained by the finite differences approach within a $(\sqrt{3}\times\sqrt{3})R30°$ structure to the experimental IR data reveals striking

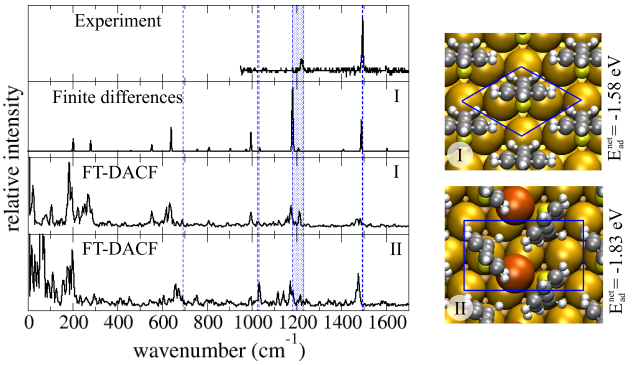

FIG. 1. Measured IR-spectrum of a BM-SAM compared with calculated spectra using the finite difference method and derived from AIMD simulations at 300 K for the $(\sqrt{3}\times\sqrt{3})R30°$ geometry (structure I) and for the energetically most favorable structure with an Au adatom in a $(3\times\sqrt{3})rect$ geometry (structure II). For comparison, the frequencies of the experimentally observed vibrational bands [13, 16, 17] are indicated as blue dashed lines. The blue shaded region corresponds to the broad band observed in the experimental high resolution electron loss spectrum [17].

discrepancies. First, the calculated spectrum, for which no scaling factor was introduced, overestimates the frequencies of the C-H stretching vibrations (not shown). This is expected due to the harmonic approximation in the simulation method. But as shown in Fig. 1 even in the mid- and low-frequency region of the IR-data theory and experiment are at variance: the simulated IR spectrum predicts the bands at around 1200 $\mathrm{cm^{-1}}$ to be the most intense ones, whereas in the experimental IR spectrum the relative intensity of these bands is much weaker. Also in earlier experimental studies reported for BM-based SAMs, these bands at 1200 $\mathrm{cm^{-1}}$ showed only a rather weak intensity [16]. In an earlier IR study [13], this mode has not been detected, possibly due to the fact that a polarization modulation was used, which may reduce intensities of bands in certain spectral regions.

A closer inspection of the modes contributing to the band at around 1200 $\mathrm{cm^{-1}}$ reveals that they are bands with strong contributions of the in-plane C-H bending motion and the wagging motion of the CH_2 group. It might be speculated that in the BM-based SAM studied experimentally different configurations of the BM radical are present, for which the transition dipole moments of these modes are orientated more parallel to the surface. However, different orientations of the thiolate species would also affect the transition dipole moments of other modes. Yet, there is good agreement between the calculated and experimental band with respect to frequencies and intensities for the in-plane C-H bending mode (calc.: 1488 $\mathrm{cm^{-1}}$ and exp.: 1492-1495 $\mathrm{cm^{-1}}$ [13, 16, 17]) and the ring-in-plane deformation mode (calc.: 1035 $\mathrm{cm^{-1}}$ and exp.: 1025-1029 $\mathrm{cm^{-1}}$ [13, 16, 17]); hence, this ex-

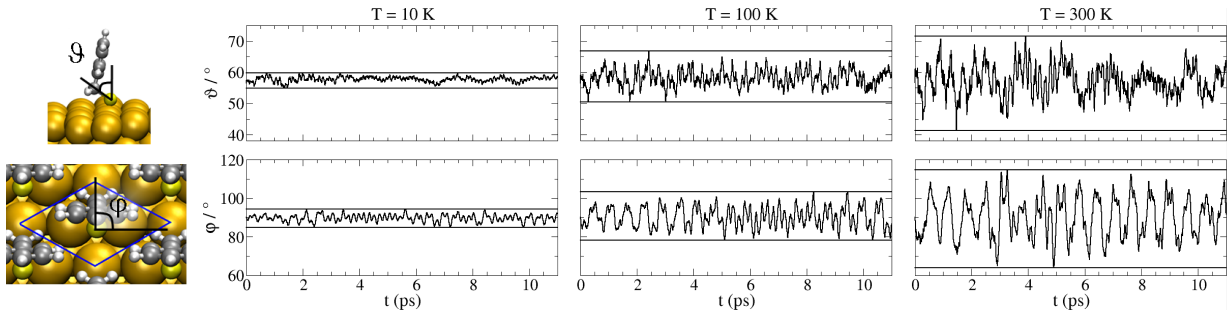

FIG. 2. Time dependent changes of the inclination (ϑ) and azimuthal (φ) angle of the S-C bond of BM adsorbed on Au(111) in a $(\sqrt{3} \times \sqrt{3})R30°$ unit cell.

planation can be ruled out.

We have furthermore checked whether considering different SAM structures could reconcile theory and experiment. A zigzag-like configuration of the SAM with two molecules in the larger $(3 \times \sqrt{3})rect$ unit cell with a T-shaped packing motif as in the bulk structure of benzene [31] is energetically slightly more favorable than the simple $(\sqrt{3} \times \sqrt{3})R30°$ overlayer structure with an all-parallel arrangement of the phenyl rings. Similar structures have also been observed in other studies of biphenyl-based SAMs [6, 32]. A further stabilization of the adsorption complex is obtained if adsorption-induced reconstructions are accounted for. Including an Au vacancy in a reconstruction motif resembling the honeycomb structure introduced for the adsorption of MeS on Au(111) [24] leads to a energy gain of 0.14 eV per BM molecule. A comparable gain in energy, 0.15 eV, is found for a structure in which two BM-radicals share one Au adatom, as in the adatom-model proposed for MeS-based SAMs [22]. However, the respective IR spectra of all these structures are rather similar. Consequently, the anomalously high intensity of the band at around 1200 cm^{-1} must have a different origin.

In order to address temperature effects, we have performed AIMD simulations of a microcanonical ensemble at various temperatures. In Fig. 2 the time-dependent changes of the structure of the BM molecule in a $(\sqrt{3} \times \sqrt{3})R30°$ structure are investigated by monitoring both the inclination (ϑ) and the azimuthal (φ) angle of the S-C bond. At 10 K, both angles do not vary by more than 10 degrees, but the variation in the angles increases to $\Delta\vartheta = 16°$ and $\Delta\varphi = 25°$ at 100 K and to $\Delta\vartheta = 30°$ and $\Delta\varphi = 51°$ at 300 K. The motion of the molecules correspond to low-energy vibrations. These frustrated rotational modes exhibit frequencies of 34 cm^{-1}(4 meV), and 96 cm^{-1}(12 meV), for variations of ϑ and at 57 cm^{-1}(7 meV) and 173 cm^{-1}(21 meV) for variations of φ. Because of the low energies, these vibrational states are indeed substantially populated at finite temperatures.

These dynamical studies demonstrate clearly, that at room temperature SAMs are by no means rigid layers

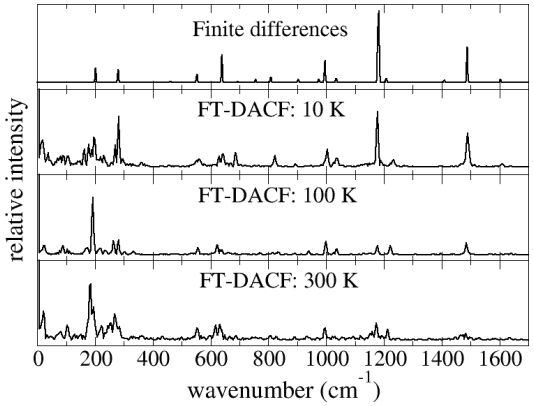

FIG. 3. The influence of temperature on vibrational spectra of BM adsorbed on Au(111) in a $(\sqrt{3} \times \sqrt{3})R30°$ unit cell is shown. The spectra have been calculated by means of the finite difference method and FT-DACF of MD simulations at different temperatures.

with fixed geometrical properties, but a rather large distribution of e.g. inclination angles can be observed. The strong variation in ϑ will also influence the orientation of the transition dipole moment of the vibrational modes relative to the surface and thus the corresponding IR-intensities. In addition, the dynamic disorder will affect the effective force-constants, leading to a change of vibrational frequencies.

This is demonstrated in Fig. 3 where the IR spectrum calculated by means of the finite difference method is compared to IR spectra obtained from a FT-DACF of AIMD simulations at different temperatures. With increasing temperature the bands at around 1200 cm^{-1} become broader. Importantly, also their intensity decreases relative to other bands originating from vibrational modes not involving a motion of the CH_2 group, such as the bands at around 1000 cm^{-1} or 1500 cm^{-1}.

Taking temperature effects in the calculated vibrational spectra into account leads to a semi-quantitative agreement between experiment and theory, as Fig. 1 con-

firms. At this level of accuracy, we are now even able to assess the structural dependence of the vibrational spectra in much more detail. In Fig. 1, which summarizes the main findings of this work, for the $(\sqrt{3} \times \sqrt{3})R30°$ geometry (structure I) the calculated IR spectra obtained from finite differences in the harmonic approximation and through FT-DACF at 300 K are compared to the FT-DACF IR spectrum at 300 K for the energetically most favorable structure with an Au adatom in a $(3 \times \sqrt{3})rect$ geometry (structure II). For structure II, the bands at around 1200 cm^{-1} are largely reduced compared to the calculated IR spectrum using the finite differences method, whilst the intensity of the bands at 1030 cm^{-1} and 1475 cm^{-1} persists. Thus the agreement between the experimental and the calculated FT-DACF IR spectrum is further improved compared to the unreconstructed surface as some of the bands are shifted closer to the experimentally observed position, e.g., the band corresponding to the S-C stretching vibration is shifted from about 630 cm^{-1} to 665 cm^{-1} (experiment: 690 cm^{-1} [17]). The band at 1030 cm^{-1} is clearly stronger than the band at 996 cm^{-1}, in contrast to the FT-DACF IR spectrum for the bulk-terminated surface, where the band at 1026 cm^{-1} is hardly visible and the band at 998 cm^{-1} is much more intense. Experimentally, there is only one band observed at around 1025-1029 cm^{-1} [13, 16, 17]. Furthermore, there is a stronger change in the transition dipole moment (and thus a stronger intensity) of the in-plane deformation mode of the phenyl-ring CH-groups (band at around 1500 cm^{-1}) if an adatom is present. With respect to the band at around 1200 cm^{-1} the intensity of the band at 1500 cm^{-1} is almost twice as large if an adatom (or vacancy) is present, again in agreement with experiment. Although still discrepancies between theory and experiment exist, it is fair to say that the room-temperature calculation of the vibrational spectra lends further credibility to the adatom-model proposed for MeS-based SAMs [22].

In conclusion, in this study we compared experimental and simulated vibrational spectra of the SAM of BM on Au(111). We observed that analogously to the conformational changes of molecules in the gas phase, the thermal excitation of frustrated rotations of chemisorbed molecules has a considerable impact on the appearance of the vibrational spectrum and has to be taken into account in order to understand the observed vibrational spectra. Furthermore, reconstruction effects upon adsorption are thermodynamically possible and the simulated vibrational spectra of a structural proposal including an Au adatom improves the comparison to experiment.

We thank the bwGRiD project for computational resources. Useful discussions with David Benoit are gratefully acknowledged.

[1] A. Ulman, Chem. Rev. **96**, 1533 (1996).
[2] F. Schreiber, Prog. Surf. Sci. **65**, 151 (2000).
[3] J. C. Love *et al.*, Chem. Rev. **105**, 1103 (2005).
[4] M. Kind and C. Wöll, Prog. Surf. Sci. **84**, 230 (2009).
[5] I. S. Ulusoy *et al.*, Phys. Chem. Chem. Phys. **13**, 612 (2011).
[6] G. Heimel *et al.*, Surf. Sci. **600**, 4548 (2006).
[7] T. Hayashi *et al.*, J. Chem. Phys. **114**, 7615 (2001).
[8] A. Nagoya and Y. Morikawa, J. Phys.: Condens. Matter **19**, 365245 (2007).
[9] X. Stammer *et al.*, Phys. Chem. Chem. Phys. **12**, 6445 (2010).
[10] D. Loffreda *et al.*, Chem. Phys. Lett. **405**, 434 (2005).
[11] J. Kučera and A. Groß, Langmuir **24**, 13985 (2008).
[12] F. Eberle *et al.*, Angew. Chem. Int. Ed. **49**, 341 (2010).
[13] K. Rajalingam *et al.*, Phys. Chem. Chem. Phys. **12**, 4390 (2010).
[14] L. H. Dubois *et al.*, J. Electr. Spectrosc. Relat. Phenom. **5455**, 1143 (1990).
[15] L. Hallmann *et al.*, Langmuir **24**, 5726 (2008).
[16] Y.-T. Tao *et al.*, Langmuir **13**, 4018 (1997).
[17] E. J. Sturrock *et al.*, J. Electr. Spectrosc. Relat. Phenom. **135**, 127 (2004).
[18] G. Kresse and J. Furthmüller, Phys. Rev. B **54**, 11169 (1996).
[19] J. P. Perdew, K. Burke, and M. Ernzerhof, Phys. Rev. Lett. **77**, 3865 (1996).
[20] P. E. Blöchl, Phys. Rev. B **50**, 17953 (1994).
[21] G. Kresse and D. Joubert, Phys. Rev. B **59**, 1758 (1999).
[22] P. Maksymovych *et al.*, Phys. Rev. Lett. **97**, 146103 (2006).
[23] M. Yu *et al.*, Phys. Rev. Lett. **97**, 166102 (2006).
[24] L. M. Molina and B. Hammer, Chem. Phys. Lett. **360**, 264 (2002).
[25] S. Grimme *et al.*, J. Chem. Phys. **132**, 154104 (2010).
[26] J. Neugebauer and M. Scheffler, Phys. Rev. B **46**, 16067 (1992).
[27] Y. Yourdshahyan and A. M. Rappe, J. Chem. Phys. **117**, 825 (2002).
[28] J. Gottschalck and B. Hammer, J. Chem. Phys. **116**, 784 (2002).
[29] N. Gonzalez *et al.*, Surf. Sci. **600**, 4039 (2006).
[30] A. Franke and E. Pehlke, Phys. Rev. B **79**, 235441 (2009).
[31] E. G. Cox *et al.*, Proc. R. Soc. A **247**, 1 (1958).
[32] W. Azzam *et al.*, Langmuir **19**, 4958 (2003).